J. Synchrotron Rad. (2000). **7**, 189–195

Precision wavelength measurement of the 14.4 keV Mössbauer photon

Zhang Xiaowei,[a]* Yoshitaka Yoda[b] and Yasuhiko Imai[c]

[a]Photon Factory, High Energy Accelerator Research Organization (KEK), Tsukuba, Ibaraki 305-0801, Japan, [b]Japan Synchrotron Radiation Research Institute (JASRI), SPring-8, Hyogo 679-5198, Japan, and [c]Department of Applied Physics, School of Engineering, University of Tokyo, Hongo, Bunkyo-ku, Tokyo 113, Japan. E-mail: zhang.xiaowei@kek.jp

(*Received 14 February 2000; accepted 7 March 2000*)

The wavelength of the 14.4 keV Mössbauer photon has been determined by using undulator radiation and diffraction of FZ silicon crystals. For the wavelength determination a goniometer equipped with a laser rotary encoder and a sine-bar angle optical interferometer was developed; a temperature-monitoring system and X-ray optics related to the experiment were also developed. The mean wavelength was 0.08602557 nm with an uncertainty of 0.6 p.p.m., derived from 16 measurements of three pieces of FZ Si(840) crystals.

Keywords: nuclear resonant scattering; Mössbauer effect; wavelength measurement.

1. Introduction

It is well known that the ratio of the line width to the $K\alpha_1$ wavelength is of the order of 10^{-4} in the X-ray range, although it is believed that the central wavelength can be determined to better than one part per million (p.p.m.). From this point of view it is clear that the characteristic X-ray line is not a good reference for a high-precision determination. The lattice parameter of Si plays a main role in the scale of the X-ray range (Cohen & Taylor, 1987), though it is well known that the lattice parameter is not an atomic quantity but a macroscopic quantity obtained from the average value of 10^{16} unit cells.

The γ-ray lines of the order of 0.1 nm would, in principle, be ideal primary wavelength standards in X-rays because of their narrow line-width, symmetric line-shape and the Mössbauer effect in solids. A feasibility study of 14.4 keV wavelength determination was carried out in the 1960s using a 200 mCi ^{57}Co γ-ray source (Bearden, 1965, 1967). Owing to the low brilliance of the γ-ray source, the measurement took a long time; the uncertainty of the determination was 25 p.p.m., poorer than that of the characteristic X-ray lines, a few p.p.m. The results of the experiment showed that, to make a γ-ray standard experimentally feasible, the intensity of the radiation source must be increased by at least a factor of 100. Synchrotron radiation from an undulator can produce a strong Mössbauer photon beam, of which the brilliance is thousands of times more intense than any isotope sources (Yamamoto *et al.*, 1993). We are now able to determine the 14.4 keV Mössbauer wavelength.

Compared with the great progress in the brilliance of X-ray sources, there has been no remarkable breakthrough in the X-ray wavelength determination, except absolute lattice parameter measurements by X-ray/optical interferometer technology (Desllates & Henins, 1973). Although a wavelength-dispersive X-ray interferometer measurement was successfully performed (Appel & Bonse, 1991), owing to the optical-path difference, which depends on both the size of the crystal interferometer and the X-ray diffraction angle, we cannot use this method to measure the X-ray wavelength accurately. The only realistic method is still utilizing the traditional crystal X-ray spectroscopy technique (Dumond & Hoyt, 1930). In this paper we describe the experimental instruments and adjustment and report on an absolute measurement of the wavelength of the 14.4 keV Mössbauer photon within an accuracy of 1 p.p.m.

2. Experimental arrangement and adjustments

A schematic view of the experimental arrangement for the wavelength measurement is shown in Fig. 1. From the left, the third-harmonic radiation from the undulator is monochromated by a beamline monochromator on beamline NE3 (Zhang *et al.*, 1992). Through an ionization chamber and a slit, the beam is succeedingly monochromated to a bandwidth of 6.5 meV at 14.4 keV by a high-resolution monochromator. The operation of the Accumulation Ring at KEK is single-bunch with a revolution of 1.2 μs. Nuclear resonant scattering events can be easily separated from those of electronic scattering using an avalanche photodiode (APD) with the combination of a time-resolved detection technique. The bandwidth was measured by nuclear resonant forward scattering from a ^{57}Fe foil, and is

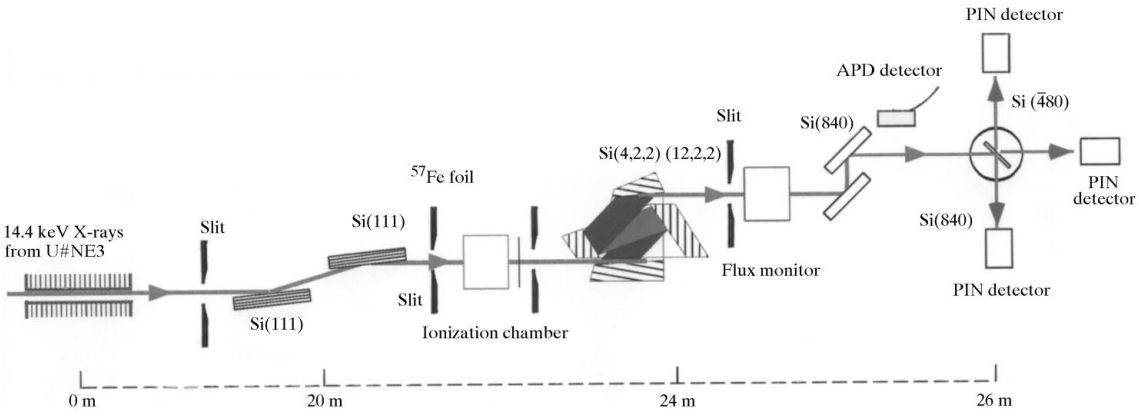

Figure 1
Schematic side view of the experimental arrangement. From the left, the undulator of beamline NE3, Si(111) beamline monochromator, a nest of 422 and 12,2,2 Si channel-cut crystals high-resolution monochromator, an 840 channel-cut beam collimator, a precision goniometer and a piece of silicon crystal. A ^{57}Fe foil and an avalanche photodiode (APD) were used for nuclear resonant scattering signal detection, and three PIN photodiodes were used for the intensity measurement of the Bragg/Laue diffractions and the transmission.

shown in Fig. 2. Because the design of the high-resolution monochromator was focused on a high throughput, the beam divergence after the beamline monochromator is about 4 arcsec, which is not suitable for a high-precision angular determination. It is necessary to add a beam collimator to the arrangement. Owing to the action of an Si(840) channel-cut collimator, the beam divergence was reduced to 0.4 arcsec, and the $\bar{4}80$ Laue and 840 Bragg diffraction were narrowed to sub-arcsec widths, as shown in Fig. 3. The final part in the illustration of the arrangement is a precision goniometer (Kohzu KTG-10) equipped with a laser rotary encoder (Canon X-1M) and an optical sine-bar small-angle measurement interferometer. Two crossed tilting stages and one rotary table are mounted on the rotary axis of the goniometer for adjusting the posture of an Si crystal. Three pieces of FZ Si(840) crystal were cut to chips of 10 mm $\times$ 40 mm, where the partial thickness of crystals for X-ray diffraction is 0.5 mm and the thickness of the mount part of the chips is 1.2 mm. The 840 atomic plane is parallel to the crystal surface within 0.05°, as illustrated in Fig. 4.

The principle of our measurement is based on the Bragg formula; the geometric relationship is shown in Fig. 4. We selected two equivalent planes, 840 and $\bar{4}80$, in one FZ Si crystal piece for X-ray diffraction. This method was proposed by Siddons *et al.* (1989) and was used in our first nuclear Bragg scattering observation experiment (Kikuta *et al.*, 1991). Because the diffraction angle of 840 for the 14.4 keV photon wavelength is 45.1°, we can find both the Bragg and the Laue diffractions within a small angle range of 0.2°. The advantage of this method is that a small angle can be determined with high precision and high accuracy; the disadvantage is that two tilt adjustments for the two diffractions of one crystal are required, which is more difficult than just tuning one.

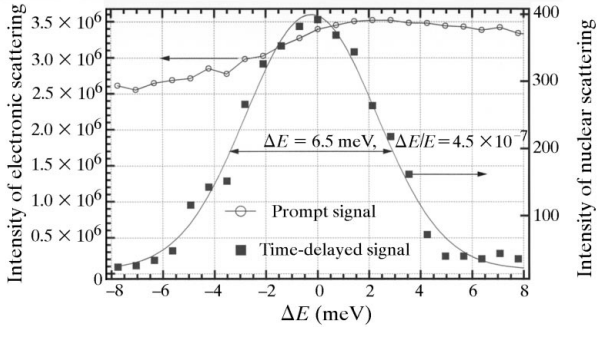

Figure 2
Bandwidth of the high-resolution monochromator. The prompt signal is electronic forward scattering, and the time-delayed signal is nuclear resonant forward scattering. The peak intensity ratio can be considered approximately corresponding to the ratio of the effective linewidth of nuclear resonant scattering to the bandwidth of the monochromator.

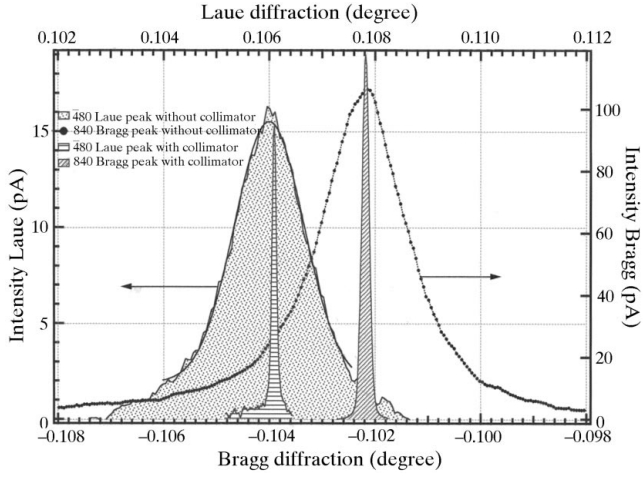

Figure 3
Rocking curves of the 840 Bragg and the $\bar{4}80$ Laue diffractions without the beam collimator (wide curves) and with the beam collimator (narrowed curves).

Let θ_L be the diffraction angle for the Laue case, and θ_B be that for the Bragg case; the 2ω angle in Fig. 4 is given by the following equation, which is the angle we should measure,

$$2\omega = 2\theta_L + 2\theta_B - 180^\circ. \quad (1)$$

After consideration, the X-ray refraction correction, $\theta_B = \theta_L + \delta/\sin 2\theta_L$ (δ is the index of refraction), the diffraction angle is given by

$$\theta_L = 45^\circ + \omega/2 - \delta/\sin 2\theta_L/2, \quad (2)$$

and the Mössbauer wavelength λ is given by

$$\lambda = 2d_{840}(t)\sin\theta_L. \quad (3)$$

Here, d_{840} is the lattice parameter of Si(840), and t is the temperature of the crystal piece.

For perfect alignment of the wavelength measurement system, (i) the rotary axis of the goniometer is set perpendicular to the X-ray beam, and (ii) the 001 direction (a common vector perpendicular to 840 and $\bar{4}80$ vectors) of the Si crystal is set parallel to the rotary axis. We narrowed the beam width to 0.3 mm, utilized a Polaroid film on a long co-axis 2θ arm of the goniometer, and checked that the first condition was satisfied within an error of 0.13 mrad. We then adjusted the two tilting stages as follows, allowing the condition (ii) to be satisfied. From Fig. 4 we know that the Laue diffraction angle should reach a maximum with the smallest width when the $\bar{4}80$ plane is adjusted to be parallel to the rotary axis, and the Bragg diffraction angle should reach a minimum (consider the sign of the Bragg angle in Fig. 4) for the 840 plane. The curves of the peak shift *versus* the tilting angle of $\bar{4}80$ and 840, in units of mrad, are shown in Fig. 5, and are consistent with the solid geometrical theory. When we adjust one tilting angle of the atomic plane, the diffraction angular position of another atomic plane could be moved, because we cannot expect that the crystal is set completely at the position where the $\bar{4}80$ and 840 planes are just perpendicular to their respective tilting stages, even with the help of the rotary table on the tilting stages. Therefore, we need an additional '2ω max-maximum condition' for complete alignment of the crystal. We considered that under this condition the common line of two atomic planes will be parallel to the rotary axis and perpendicular to the X-ray beam. After the process of adjusting two tilting stages, shown in Fig. 5, we measured the 2ω angle *versus* the tilting angles of 840 and $\bar{4}80$, as shown in Fig. 6. Because the configuration of the 840 Bragg diffraction is a (+,+) arrangement to the collimator, where the wavelength is sensitive to the Bragg angular position, the top of the 2ω curve is located at -15.3 mrad, which was slightly different from that of the Bragg peak at -16.3 mrad shown in Fig. 5. For the (+,−) arrangement of $\bar{4}80$ Laue diffraction, where the wavelength *versus* the diffraction angle is not as sensitive as the (+,+) arrangement, the top

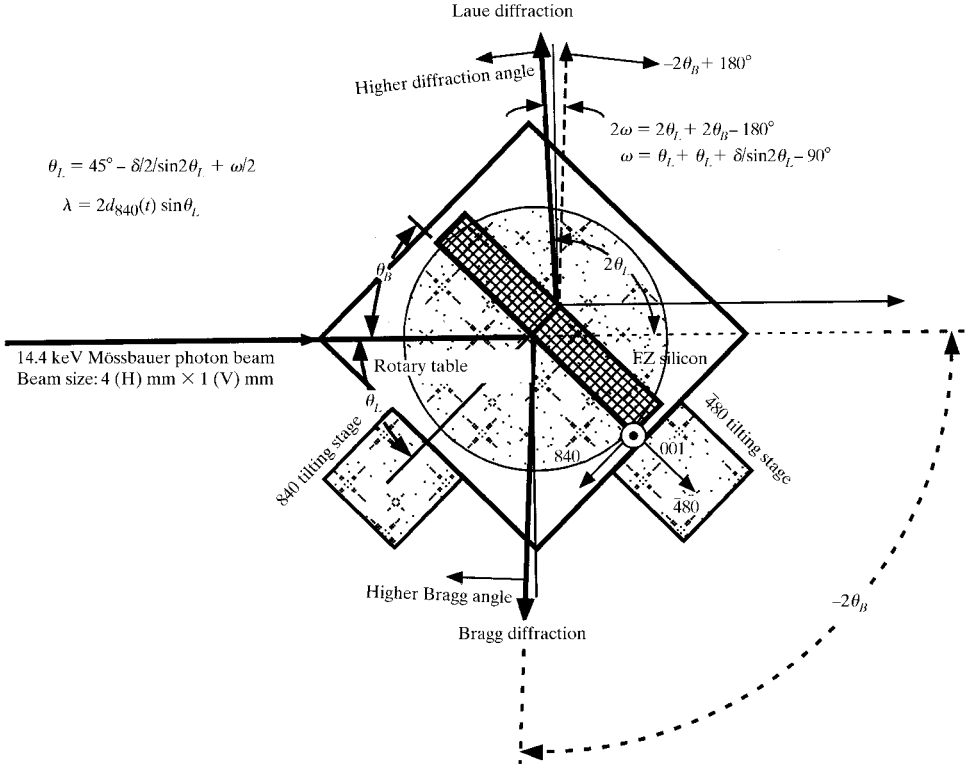

Figure 4
Laue beam diffracted upwards with a scattering angle of $2\theta_L$, and the Bragg beam reflected downwards with an angle of $2\theta_B$. The diffraction angle can be derived from a measurement of 2ω and the δ index of refraction. The rotary table is used to adjust the Si piece position; let 840 and $\bar{4}80$ atomic planes be parallel to their tilting stages.

Table 1
Wavelength measurement by three pieces of 840 FZ silicon.

Crystal and direction		2ω (°)	θ_L (°)	t (K)	λ (nm)
1	1 cw	0.204595	45.102164	298.39	0.086025548
	2 ccw	0.204602	45.102167	298.39	0.086025553
	3 cw	0.204619	45.102175	298.39	0.086025566
	4 ccw	0.204604	45.102168	298.39	0.086025554
2	5 cw	0.204607	45.102170	298.48	0.086025576
	6 ccw	0.204609	45.102171	298.48	0.086025578
	7 cw	0.204608	45.102170	298.48	0.086025577
	8 ccw	0.204607	45.102169	298.48	0.086025576
	9 cw	0.204608	45.102170	298.48	0.086025577
	10 ccw	0.204605	45.102169	298.48	0.086025575
3	11 cw	0.204606	45.102169	298.43	0.086025565
	12 ccw	0.204608	45.102170	298.43	0.086025566
	13 cw	0.204603	45.102168	298.43	0.086025562
	14 ccw	0.204605	45.102169	298.43	0.086025564
	15 cw	0.204606	45.102169	298.43	0.086025565
	16 ccw	0.204608	45.102170	298.43	0.086025566
Average					0.086025567
σ					0.0000000095

position of the 2ω curve was consistent with that of the Laue peak curve shown in the graph.

3. Temperature monitor system and angular measurement equipment

The temperatures of the crystals and the experimental environment were monitored by six platinum and three thermistor sensors. The accuracy of a standard platinum 25 Ω resistance thermometer (Chino/R800-2, serial No. RS96Z-3) is 0.01 K (with an AZONIX controller); other sensors were calibrated by the standard sensor at the melting points of ice and gallium. The temperatures of the high-resolution monochromator, atmosphere and holder of the Si(840) crystal were recorded every 10 s during the experiment. A section of the record chart is shown in Fig. 7. The temperature readings from the standard thermometer and a mini-Pt sensor, which were used to monitor the atmosphere of the crystal, are in between that of the two temperatures of the crystal holder. We considered that the true temperature of the crystal should be a value between them. The temperature fluctuation with an amplitude of 0.01 K and a period of 23 min recorded by the atmosphere monitors was due to the air conditioner in the experimental hall.

We assembled the optical sine-bar angular measurement system by mounting two one-inch cube-corners (Edmund Scientific) on a super-invar frame (Marzolf, 1964), and measured the angular displacement by a commercial laser metric system (HP 5529A dynamic calibrator). The bar length was calibrated in the ±3.5° angular range and 281 measurement points by the X-1M rotary encoder equipped on a precision goniometer. One of the calibration measurements, its sin-fitting curve and the residuals are shown in Fig. 8. The average of the bar length is 140.2030 ± 0.0006 mm (5 p.p.m., 1σ), which corresponds to the accuracy of the X-1M encoder, 1 arcsec in 360°. Using the sine-bar interferometer angular measurement system, we can measure 0.1° with an accuracy of 10 p.p.m. (2σ). When we convert this accuracy into a Bragg angle of 45°, the accuracy of the angular determination is better than 0.1 p.p.m.

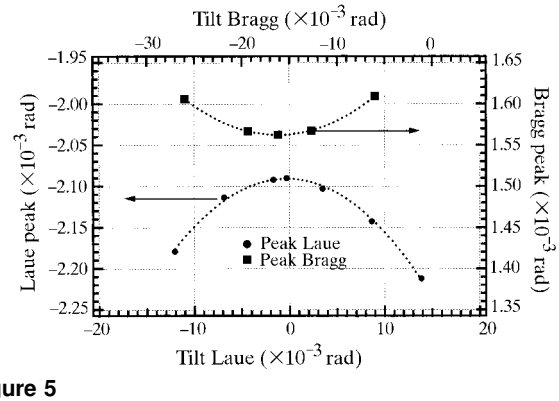

Figure 5
Diffraction peak shifts *versus* their tilting angles. The curve of the Laue peak gives the maximum diffraction angle, and the curve of the Bragg peak gives the minimum diffraction angle at their optimized tilting positions. The dashed lines are a parabola curve fitting.

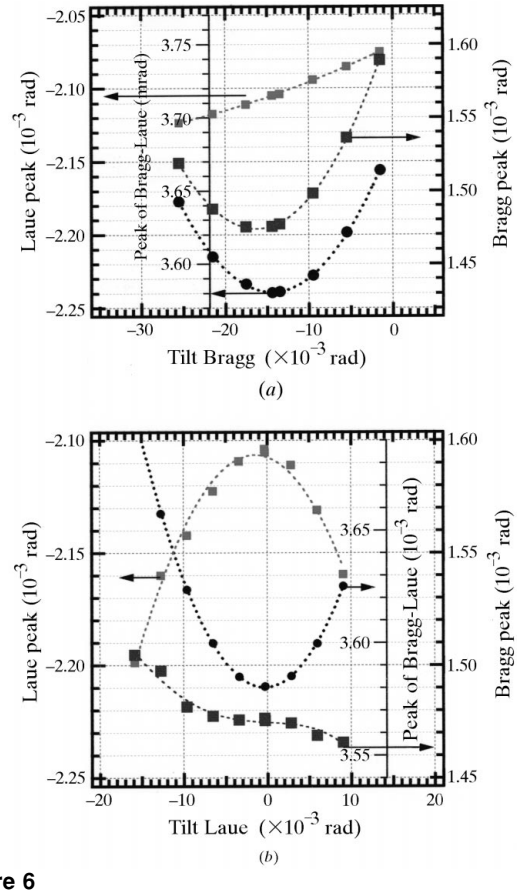

Figure 6
2ω angle (circle) *versus* tilting angle of the Bragg (*a*) and the Laue (*b*) diffractions. For the $\bar{4}80$ Laue tilting angle the position of maximum 2ω angle is −0.05 mrad, consistent with that in Fig. 5; for the 840 Bragg tilting angle the top of the 2ω curve is −15.3 mrad, slightly different from the value of −16.3 mrad in Fig. 5.

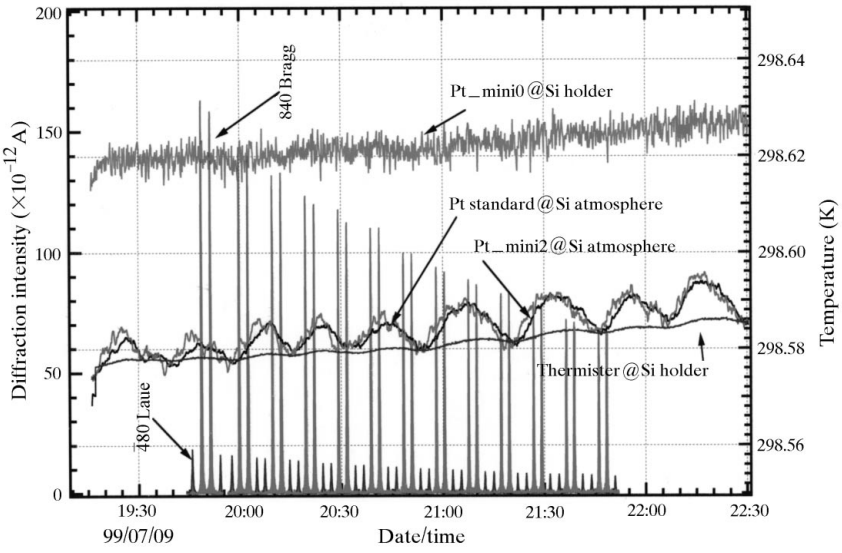

Figure 7
Sector of the temperature chart during the experiment. Four thermometers were used to monitor the temperature of the Si(840) crystal. A Pt_mini0 probe and a thermistor were mounted in the crystal holder, and the Pt standard thermometer and Pt_mini2 probe were located near to the crystal, monitoring the atmosphere of the sample. The angle measurement of the Laue and the Bragg diffraction were also recorded. The decay of the diffraction intensity corresponded to that of the ring current.

4. Discussion of experimental results

One pair of measurements of the 840 Bragg and the $\bar{4}80$ Laue electronic diffractions are shown in Fig. 9. Because the intensity of the nuclear signal is not sufficiently strong at beamline NE3, the curves in Fig. 9 were not directly measured by the time-delayed nuclear signal. However, this is not essential for the wavelength determination. Because the bandwidth of the X-ray is sub-p.p.m., which is satisfactory for the precision we need, we also confirmed that the centre of the nuclear resonant signal was identical to that of the electronic signal before and after every measurement circle by rocking the collimator as in the plot in Fig. 10.

Sixteen measurement results obtained from three 840 Si pieces are listed in Table 1. The first column is the crystal code, measurement direction and order; the second column is the angle of 2ω in degrees observed by the sine-bar angular-measurement system. The third column is the Laue diffraction angle obtained by equation (2) with $\delta/\sin 2\theta_L = 4.672 \times 10^{-6}$ (Sasaki, 1989). The fourth column is the temperature of the crystal obtained from the average of two readings of the crystal holder and one reading from the atmosphere. The last column is the wavelength obtained using equation (3) with an Si lattice parameter of 0.543101773 nm (1 atm, 295.5 K; Cohen & Taylor, 1986) and the coefficient of thermal expansion $\alpha(t) = 2.56 \times 10^{-6}\,\mathrm{K}^{-1}$ (298 K; Okada & Tokumaru, 1984). The average of the 16 measurements is 0.08602557 nm and its standard deviation is 9.5×10^{-9} nm, corresponding to a relative deviation of 0.1 p.p.m., which means that the reproducibility of our measurements was very good.

The errors in our measurements were estimated to be as follows, and are listed in Table 2. Because $\Delta\lambda/\lambda = \Delta d/d \sin\theta_L + \cot\theta_L \Delta\theta_L$, the uncertainty in the wavelength

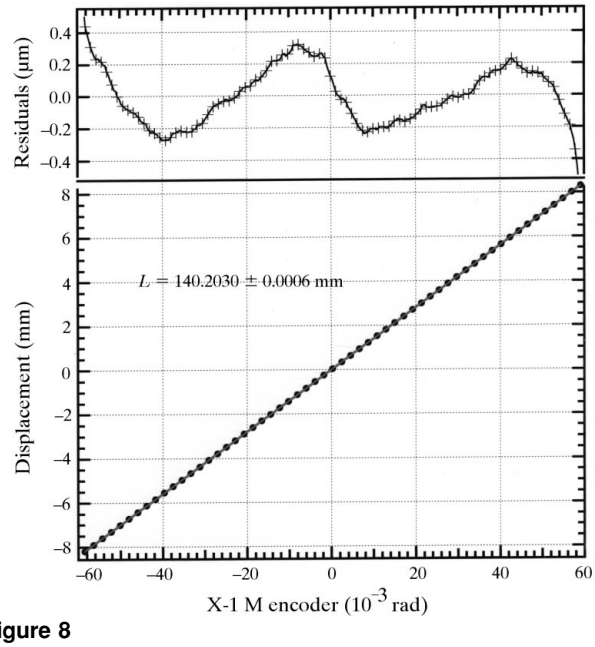

Figure 8
Calibration of the length of the optical sine-bar. The filled circles and the line are measurement points and sine-curve fitting, respectively. The displacement of the sine-bar was measured by HP 5529A (laser metric system) to an accuracy of 0.1 p.p.m. and a resolution of 1 nm. The X-1M rotary encoder is assembled on the Kohzu KTG-10 goniometer without any coupler. The accuracy of the encoder is smaller than 1 arcsec in 360°, and the resolution of the encoder is 0.0056 arcsec with the IU-1000 interpolator. The average length of the sine-bar is 140.2030 ± 0.0006 mm, obtained from four bi-directional measurements.

Table 2
Errors in the measurement and wavelength determination.

Error source		Error	$\Delta\lambda/\lambda$ (p.p.m.)
$\Delta d/d$	1 Lattice spacing	<0.21 p.p.m.	0.21
	2 Crystal temperature	<0.1 K	0.26
$\Delta\theta_L$	1 Perpendicularity of goniometer axis	<0.13 mrad	0.016
	2 Tilts of 840 and $\bar{8}40$	<0.07 mrad	0.005
	3 Determination of 2ω	<10 p.p.m.	0.02
	4 Refraction index	<0.01 μrad	0.01
	5 Absorption	<0.045 μrad	0.05
	6 Beam divergence and slit width	<0.08 mrad	0.016
	7 Polarization	–	–
	8 Asymmetry factor	–	–
Sum			0.59

determination arises from two parts. The first part relates to the lattice parameter and temperature of the silicon crystal, contributing to 0.5 p.p.m. in the uncertainty, which is five times larger than the measurement reproducibility. The second part arises from a determination of the diffraction angle. Although there are many factors in this term, as shown in Table 2, we estimated that the uncertainty due to this part is only 0.1 p.p.m., smaller than the first part. The total uncertainty was estimated to be 0.6 p.p.m. (2σ).

In conclusion, we have plotted in Fig. 11 the previous and present 14.4 keV wavelength and their uncertainties. The present value is 4.5 p.p.m. larger than Bearden's original (Bearden, 1965, 1967) with the old Å* to Å conversion factor given in 1967, which corresponds to 0.8602516 Å. The recommended conversion factor in 1986 was reduced by a factor of 5.7 p.p.m. compared with the old one. Under the new conversion ratio our result is 10 p.p.m. larger than Bearden's. The present value is 7 p.p.m. lower than Siddons' result (Siddons *et al.*, 1988), measured 11 years ago using an Si(10,6,4) crystal with synchrotron radiation, and near to our early experimental result obtained using beamline 14B, a vertical wiggler beamline on the 2.5 GeV

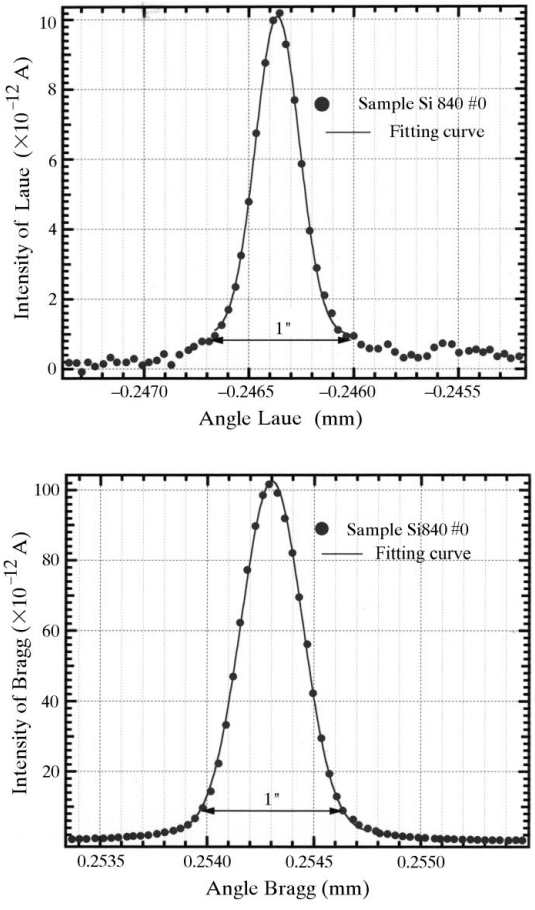

Figure 9
Rocking curves of $\bar{4}80$ Laue scattering (top) and 840 Bragg scattering (bottom) measured by the HP 5529A laser metric system. Because of the (+,+) arrangement of the 840 Bragg diffraction, the width of the Bragg curve is slightly wider than that of the Laue diffraction.

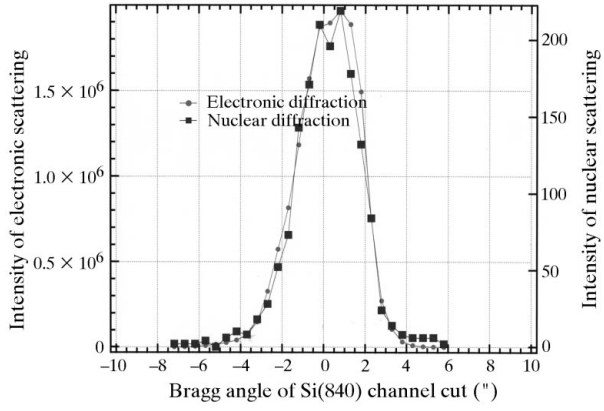

Figure 10
Rocking curve of the Si(840) channel-cut beam collimator. The filled squares represent nuclear resonant scattering and the filled circles represent electronic scattering. The peak positions of two curves are consistent during the experiment.

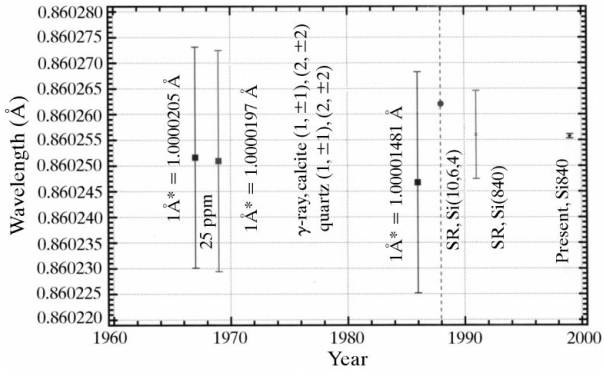

Figure 11
The published 14.4 keV wavelength and their uncertainties. The three filled squares and their error bars are Bearden's results with different Å* to Å conversion factors in 1967, 1969 and 1986. His measurement was carried out in the 1960s using a γ-ray source and crystals of calcite and quartz. The filled circle in 1988 is Siddon's result without uncertainty information. The values in 1991 and 1999 are our results with uncertainties of 10 p.p.m. and 0.6 p.p.m., respectively. The measurements after the 1980s were carried out using synchrotron radiation and silicon crystals.

ring of the Photon Factory. The uncertainty of the 14.4 keV wavelength is reduced from Bearden's 25 p.p.m. to the present experiment of 0.6 p.p.m. For higher-precision wavelength measurements we should develop X-ray interferometer technology, where the wavelength in the X-ray range can be directly compared with visible light.

References

Appel, A. & Bonse, U. (1991). *Phys. Rev. Lett.* **67**, 1673–1677.

Bearden, J. A. (1965). *Phys. Rev.* **137**, B455–461.

Bearden, J. A. (1967). *Rev. Mod. Phys.* **39**, 78–124.

Cohen, R. E. & Taylor, B. N. (1987). *Rev. Mod. Phys.* **59**, 1121–1148.

Desllates, R. D. & Henins, A. (1973). *Phys. Rev. Lett.* **31**, 972–976.

Dumond, J. W. & Hoyt, A. (1930). *Phys. Rev.* **36**, 1702–1720.

Kikuta, S., Yoda, Y., Kudo, Y., Izumi, K., Ishikawa, T., Suzuki, C. K., Ohno, H., Takei, H., Nakayama, K., Zhang, X. W., Matushita, T., Kishimoto, S. & Ando, M. (1991). *J. Appl. Phys.* **30**, L1686–1688.

Marzolf, J. G. S. J. (1964). *Rev. Sci. Instrum.* **35**, 1212–1215.

Okada, Y. & Tokumaru, Y. (1984). *J. Appl. Phys.* **56**, 314–320.

Sasaki, S. (1989). Report 88–14. KEK, Tsukuba, Ibaraki 305, Japan.

Siddons, D. P., Hastings, J. B. & Faigel, G. (1988). *Nucl. Instrum. Methods*, A**266**, 329–335.

Siddons, D. P., Hastings, J. B., Faigel, G., Grover, J. R., Haustein, P. E. & Berman, L. E. (1989). *Rev. Sci. Instrum.* **60**, 1649.

Yamamoto, S., Zhang, X. W., Kitamura, H., Shioya, T., Mochizuki, T., Sugiyama, H., Ando, M., Yoda, Y., Kikuta, S. & Takei, J. (1993). *J. Appl. Phys.* **74**, 500–503.

Zhang, X. W., Mochizuki, T., Sugiyama, H., Yamamoto, S., Kitamura, H., Shioya, T., Ando, M., Yoda, Y., Ishikawa, T., Kikuta, S. & Suzuki, C. K. (1992). *Rev. Sci. Instrum.* **63**, 404–407.